Advanced Robotics, Vol. 15, No. 7, pp. 711–728 (2001)

Full paper

Motion control of a two-wheeled mobile robot

TAKATERU URAKUBO *, KAZUO TSUCHIYA and KATSUYOSHI TSUJITA

Department of Aeronautics and Astronautics, Graduate School of Engineering, Kyoto University, Yoshida-honmachi, Sakyo-ku, Kyoto 606-8501, Japan

Received 29 September 2000; accepted 14 December 2000

Abstract—The design of the controller of a two-wheeled mobile robot is usually based on a kinematical model. The kinematical model is derived under the assumption that the wheels do not skid or float. However, in the real world, wheels may skid on the ground or float away from the ground due to the rotational motion of the body. This paper analyzes the effects of the skid and the float on the robot with a controller designed based on the kinematical model — by the use of the Lyapunov control method. Numerical simulations are carried out based on the dynamic model including the translational and rotational motion of the body, and then experiments are performed using a hardware model.

Keywords: Non-holonomic system; kinematic model; dynamic model; Lyapunov control; experiments.

1. INTRODUCTION

One of the basic functions of a robot is mobility and mobile robots have mechanisms such as legs or wheels to realize the mobility. For this kind of robot, the motion can be determined by the kinematic constraints between the degrees of freedom of motion of the mechanism. For a wheeled robot, when the wheels do not skid or float, the motion is determined by the angles of rotation of the wheels. This kind of dynamic system is called a non-holonomic system. The controller for a non-holonomic system can be designed based on the kinematic constraints. A wheeled robot is a non-holonomic system and the controller for the wheeled robot can be designed based on the kinematic constraints. A wheeled robot does not always satisfy the kinematic constraints. The wheels often skid on the ground or float away from the ground according to the rolling motion of the body. When the motion controller for the wheeled robot is designed based on the kinematic model, it is

*To whom correspondence should be addressed. E-mail: urakubo@kuaero.kyoto-u.ac.jp

important to examine the dynamic effect of the motion, the skid and the float of the wheels.

Several controllers for a two-wheeled mobile robot have already been proposed. Those controllers are designed based on a kinematical model and are classified as time-varying controllers and discontinuous time-invariant controllers. Time-varying controllers was originated by Samson [1]. Sørdalen and Egeland [2] and M'Closkey and Murray [3] proposed non-smooth time-varying controllers which provide exponential rates of convergence. Discontinuous time-invariant feedback controllers have been proposed, such as the controller proposed by Khennouf and Canudas de Wit [4]. Astolfi proposed a method of designing a controller by transforming an original system through a non-smooth coordinate transformation and designing a smooth time-invariant controller for the transformed system [5, 6]. The controllers provide exponential rates of convergence.

On the other hand, some experiments have been performed to check the robustness of the controller [7–9]. Astolfi has performed an experiment for a two-wheeled mobile robot with a discontinuous controller [6]. M'Closkey and Murray have performed an experiment for a mobile robot towing a trailer with a time-varying controller [10]. In these experiments, the robustness against measurement noise or model errors in the kinematic model is checked. There have been few investigations which take account of the skid and the float of the wheels to check the validity of the kinematic model.

In this paper, we design a controller for a two-wheeled mobile robot based on a kinematical model, and check the effect of the skid and the float of the wheels on the control performance by numerical simulations and experiments. The controller is designed by extending the Lyapunov method. First, we define a positive-definite function (Lyapunov function) which is minimized at the desired point. Then, we construct a tensor by superposing an asymmetric tensor on a symmetric positive-definite tensor and design the control input by multiplying the gradient vector of the Lyapunov function by the tensor. The designed controller is a discontinuous time-invariant feedback controller. Experiments are carried out to check the dynamic effect of the motion, the skid and the float of the wheels on the control performance. The paper is organized as follows. We derive a dynamic model of a two-wheeled mobile robot. This model implies the translational motion with 3 d.o.f. and the rotational motion with 3 d.o.f. of the body, and also implies the effect of the skid and the float of the wheels. The dynamic model is transformed into a kinematical model under certain assumptions. Then, we design a controller with the kinematic model and analyze the behavior of the controlled system by numerical simulations based on the dynamic model and experiments.

2. A DYNAMIC MODEL OF A TWO-WHEELED MOBILE ROBOT

We consider a symmetrical two-wheeled mobile robot composed of three rigid links, the body and two wheels, as shown in Fig. 1. We that a rigid bar is attached on the

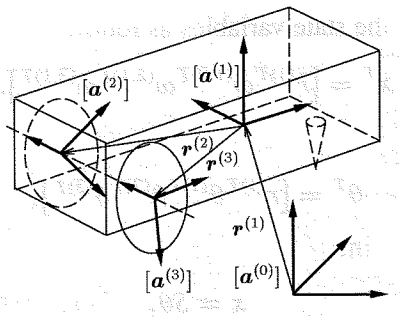

Figure 1. Schematic model of a two-wheeled mobile robot.

front of the body so that the body is kept horizontal on the ground and also assume that the rigid bar slips smoothly on the ground. Each wheel is driven by its own motor torque and touches the ground at a point. Frictional forces act on the points of the wheels. We will derive an equation of motion of the two-wheeled mobile robot. The model implies the translational motion with 3 d.o.f. and the rotational motion with 3 d.o.f. of the body and the rotational motion with 1 d.o.f. of each wheel.

The body, the left wheel and the right wheel are labeled as link 1, 2 and 3. We introduce a set of unit vectors $\{\boldsymbol{a}^{(0)}\} = \{\boldsymbol{a}_1^{(0)}\boldsymbol{a}_2^{(0)}\boldsymbol{a}_3^{(0)}\}$ fixed in an inertia space and a set of unit vectors $\{\boldsymbol{a}^{(i)}\} = \{\boldsymbol{a}_1^{(i)}\boldsymbol{a}_2^{(i)}\boldsymbol{a}_3^{(i)}\}$ fixed in link i. The origin of $\{\boldsymbol{a}^{(1)}\}$ is the total mass center of the three links and the origin of $\{\boldsymbol{a}^{(i)}\}$ is the mass center of the link i $(i = 2, 3)$. The direction of $\boldsymbol{a}_1^{(1)}$ is toward the front of the body and the direction of $\boldsymbol{a}_3^{(1)}$ is toward the top of the body. The direction of $\boldsymbol{a}_2^{(i)}$ $(i = 1, 2, 3)$ coincides with the direction of the rotation axis of the wheels. Using these sets of unit vectors, we define the following column matrices:

$$[\boldsymbol{a}^{(0)}]^T = [\boldsymbol{a}_1^{(0)}\boldsymbol{a}_2^{(0)}\boldsymbol{a}_3^{(0)}]$$
$$[\boldsymbol{a}^{(1)}]^T = [\boldsymbol{a}_1^{(1)}\boldsymbol{a}_2^{(1)}\boldsymbol{a}_3^{(1)}]$$
$$[\boldsymbol{a}^{(i)}]^T = [\boldsymbol{a}_1^{(i)}\ \boldsymbol{a}_2^{(i)}\ \boldsymbol{a}_3^{(i)}] \quad (i = 2, 3).$$

We introduce the following vectors:

$\boldsymbol{\omega}^{(k,l)}$: angular velocity of $\{\boldsymbol{a}^{(k)}\}$ with respect to $\{\boldsymbol{a}^{(l)}\}$
$\boldsymbol{\omega}^{(k,l)} = [\boldsymbol{a}^{(k)}]^T\,\omega^{(k,l)}$

$\boldsymbol{r}^{(1)}$: position vector from the origin of $\{\boldsymbol{a}^{(0)}\}$ to the origin of $\{\boldsymbol{a}^{(1)}\}$
$\boldsymbol{r}^{(1)} = [\boldsymbol{a}^{(0)}]^T r^{(1)}$

$\boldsymbol{r}^{(i)}$: position vector from the origin of $\{\boldsymbol{a}^{(1)}\}$ to the origin of $\{\boldsymbol{a}^{(i)}\}$ $(i = 2, 3)$
$\boldsymbol{r}^{(i)} = [\boldsymbol{a}^{(1)}]^T r^{(i)}$,

where the equation $\boldsymbol{b} = [\boldsymbol{a}^{(i)}]^T b$ defines b as the expression of the vector $\boldsymbol{b}$ in the frame $\{\boldsymbol{a}^{(i)}\}$. The following coordinate transform matrices are defined:

$A^{(k,l)}$: a coordinate transform matrix from $\{\boldsymbol{a}^{(k)}\}$ to $\{\boldsymbol{a}^{(l)}\}$.

We express the orientation of $\{\boldsymbol{a}^{(1)}\}$ with respect to $\{\boldsymbol{a}^{(0)}\}$ as Euler 1–2–3 angles $\theta^{(1)}$ and the orientation of $\{\boldsymbol{a}^{(i)}\}$ with respect to $\{\boldsymbol{a}^{(1)}\}$ as Euler 1–2–3 angles $\theta^{(i)}$

($i = 2, 3$). We introduce the state variables as follows:

$$x^T = \left[\dot{r}^{(1)T}\omega^{(1,0)T}\omega^{(2,1)T}\omega^{(3,1)T}\right]. \tag{1}$$

When the variable:

$$\theta^T = \left[r^{(1)T}\theta^{(1)T}\theta^{(2)T}\theta^{(3)T}\right], \tag{2}$$

is also introduced, we obtain:

$$x = S\dot{\theta}, \tag{3}$$

where:

$$S = \begin{bmatrix} I & \mathbf{0} & \mathbf{0} & \mathbf{0} \\ \mathbf{0} & S_3(\theta_3^{(1)})S_2(\theta_2^{(1)}) & \mathbf{0} & \mathbf{0} \\ \mathbf{0} & \mathbf{0} & I & \mathbf{0} \\ \mathbf{0} & \mathbf{0} & \mathbf{0} & I \end{bmatrix},$$

$$S_2(\theta) = \begin{bmatrix} \cos\theta & 0 & 0 \\ 0 & 1 & 0 \\ \sin\theta & 0 & 1 \end{bmatrix},$$

$$S_3(\theta) = \begin{bmatrix} \cos\theta & \sin\theta & 0 \\ -\sin\theta & \cos\theta & 0 \\ 0 & 0 & 1 \end{bmatrix},$$

I : 3×3 unit matrix,
$\mathbf{0}$: 3×3 zero matrix.

The kinetic energy T of the total system is expressed as:

$$2T = x^T H^T \left(\hat{\mathcal{L}}^T M \hat{\mathcal{L}} + J\right) H x, \tag{4}$$

where:

$$\hat{\mathcal{L}} = \begin{bmatrix} \mathbf{0} & \mathbf{0} & \mathbf{0} & \mathbf{0} \\ A^{(1,0)} & \mathbf{0} & \mathbf{0} & \mathbf{0} \\ A^{(2,0)} & A^{(2,1)}\tilde{r}^{(2)} & \mathbf{0} & \mathbf{0} \\ A^{(3,0)} & A^{(3,1)}\tilde{r}^{(3)} & \mathbf{0} & \mathbf{0} \end{bmatrix}, \tag{5}$$

$$H = \begin{bmatrix} I & \mathbf{0} & \mathbf{0} & \mathbf{0} \\ \mathbf{0} & I & \mathbf{0} & \mathbf{0} \\ \mathbf{0} & A^{(2,1)} & I & \mathbf{0} \\ \mathbf{0} & A^{(3,1)} & \mathbf{0} & I \end{bmatrix}, \tag{6}$$

$$M = \begin{bmatrix} \mathbf{0} & \mathbf{0} & \mathbf{0} & \mathbf{0} \\ \mathbf{0} & m^{(1)}I & \mathbf{0} & \mathbf{0} \\ \mathbf{0} & \mathbf{0} & m^{(2)}I & \mathbf{0} \\ \mathbf{0} & \mathbf{0} & \mathbf{0} & m^{(3)}I \end{bmatrix}, \tag{7}$$

$$J = \begin{bmatrix} \mathbf{0} & \mathbf{0} & \mathbf{0} & \mathbf{0} \\ \mathbf{0} & J^{(1)} & \mathbf{0} & \mathbf{0} \\ \mathbf{0} & \mathbf{0} & J^{(2)} & \mathbf{0} \\ \mathbf{0} & \mathbf{0} & \mathbf{0} & J^{(3)} \end{bmatrix}, \tag{8}$$

and we use the following quantities:

$m^{(1)}$: mass of the body,
$m^{(i)}$: mass of the wheel i, $m^{(2)} = m^{(3)}$,
$J^{(1)}$: inertia matrix of the body about the origin of $\{\boldsymbol{a}^{(1)}\}$ expressed in the frame $\{\boldsymbol{a}^{(1)}\}$,
$J^{(i)}$: inertia matrix of the wheel i about the origin of $\{\boldsymbol{a}^{(i)}\}$ expressed in the frame $\{\boldsymbol{a}^{(i)}\}$ $(i = 2, 3)$.

For a vector $h^T = [\, h_1 \,,\ h_2 \,,\ h_3 \,]$, a matrix $\tilde{h}$ is defined as follows:

$$\tilde{h} = \begin{bmatrix} 0 & h_3 & -h_2 \\ -h_3 & 0 & h_1 \\ h_2 & -h_1 & 0 \end{bmatrix}.$$

The generalized momentum $\hat{L}$ for the state variable x is computed as:

$$\hat{L} = \begin{bmatrix} \hat{L}^{(0)} \\ \hat{L}^{(1)} \\ \hat{L}^{(2)} \\ \hat{L}^{(3)} \end{bmatrix} = \left(\frac{\partial T}{\partial x}\right)^T + \left(\frac{\partial T}{\partial x^T}\right)$$
$$= H^T\left(\hat{\mathcal{L}}^T M \hat{\mathcal{L}} + J\right) H x. \tag{9}$$

The components of $\hat{L}$ are physically interpreted as

$\hat{L}^{(0)}$: translation momentum of the total system expressed in the frame $\{\boldsymbol{a}^{(0)}\}$
$\hat{L}^{(1)}$: angular momentum of the total system about the origin of $\{\boldsymbol{a}^{(1)}\}$ expressed in the frame $\{\boldsymbol{a}^{(1)}\}$
$\hat{L}^{(i)}$: angular momentum of the wheel i about the origin of $\{\boldsymbol{a}^{(i)}\}$ expressed in the frame $\{\boldsymbol{a}^{(i)}\}$ $(i = 2, 3)$.

Using $\hat{L}$, the equation of motion is derived as follows:

$$\dot{\hat{L}} + \Omega \hat{L} = \hat{G}, \tag{10}$$

where:

$$\Omega = \begin{bmatrix} \mathbf{0} & \mathbf{0} & \mathbf{0} & \mathbf{0} \\ \mathbf{0} & \tilde{\omega}^{(1,0)T} & \mathbf{0} & \mathbf{0} \\ \mathbf{0} & \mathbf{0} & \tilde{\omega}^{(2,0)T} & \mathbf{0} \\ \mathbf{0} & \mathbf{0} & \mathbf{0} & \tilde{\omega}^{(3,0)T} \end{bmatrix}, \tag{11}$$

and $\hat{G}$ is a generalized force expressed as:

$$\hat{G}^T = \left[\hat{G}^{(0)T}\ 0\ 0\ 0\ \hat{G}^{(2)T}\ \hat{G}^{(3)T}\right], \tag{12}$$

$$\hat{G}^{(0)T} = \left(m^{(1)} + m^{(2)} + m^{(3)}\right)[0, 0, g_0],$$

$$\hat{G}^{(i)T} = \left[\tau_1^{(i)}, \tau_2^{(i)}, \tau_3^{(i)}\right] \quad (i = 2, 3),$$

where g_0 is the gravity force acting on the unit mass and $\tau_2^{(i)}$ is torque to drive the wheel i.

Two types of kinematic constraints for the system are considered. One is the constraint that a wheel or the bar on the body does not float away from the ground. We express this type of constraints as $\Phi = 0$. The other is the constraint that a wheel does not skid on the ground. We express this type of constraints as $\Psi = 0$.

$$\Phi = \begin{bmatrix} \Phi_3^{(1)}(\theta) \\ \Phi_3^{(2)}(\theta) \\ \Phi_3^{(3)}(\theta) \end{bmatrix} = 0, \quad \Psi = \begin{bmatrix} \Psi_1^{(2)}(\theta, x) \\ \Psi_2^{(2)}(\theta, x) \\ \Psi_1^{(3)}(\theta, x) \\ \Psi_2^{(3)}(\theta, x) \end{bmatrix} = 0. \tag{13}$$

If the constraints are satisfied, the constraints and the equation of motion (10) are put together by the method of Lagrange undetermined multiplier:

$$\dot{\hat{L}} + \Omega\hat{L} = \hat{G} + \left(E^T S^{-1}\right)^T \Gamma_\Phi + K\Lambda_\Psi, \tag{14}$$

where:

$$E^T = \frac{\partial \Phi}{\partial \theta}, \quad K^T = \frac{\partial \Psi}{\partial x}, \tag{15}$$

and Γ_Φ and Λ_Ψ are Lagrange undetermined multipliers. The motion of the two-wheeled mobile robot is determined by the equation of motion (14) and the constraints (13).

3. DESIGN OF A CONTROLLER

3.1. Basic equation for the design of a controller

We assume that the wheels and the bar do not float away from the ground, and that the wheels of the two-wheeled mobile robot do not skid at all. Then, translational velocity u_1 and angular velocity u_2 of the mobile robot are determined by the following kinematic relationship:

$$\begin{bmatrix} u_1 \\ u_2 \end{bmatrix} = \begin{bmatrix} D/2 & D/2 \\ -D/R & D/R \end{bmatrix} \begin{bmatrix} \dot{\theta}_2^{(2)} \\ \dot{\theta}_2^{(3)} \end{bmatrix}, \tag{16}$$

where D is the radius of each wheel and R is the distance between the two wheels. We consider the following feedback law of the torque $\tau_2^{(i)}$ to the wheel i:

$$\begin{bmatrix} \tau_2^{(2)} \\ \tau_2^{(3)} \end{bmatrix} = -K_t \left(\begin{bmatrix} \dot{\theta}_2^{(2)} \\ \dot{\theta}_2^{(3)} \end{bmatrix} - \begin{bmatrix} D/2 & D/2 \\ -D/R & D/R \end{bmatrix}^{-1} \begin{bmatrix} \hat{u}_1 \\ \hat{u}_2 \end{bmatrix} \right), \tag{17}$$

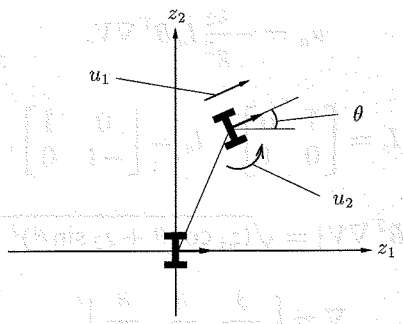

Figure 2. State variables, z_1, z_2 and θ, and inputs, u_1 and u_2, of a two-wheeled mobile robot.

where K_t is a constant, and $\hat{u}_1$ and $\hat{u}_2$ are given reference velocities. When the feedback gain K_t is large, translational velocity u_1 and angular velocity u_2 of the mobile robot follow the reference velocities quickly. In that case, we assume that translational velocity u_1 and angular velocity u_2 of the mobile robot can be arbitrarily manipulated and regarded as the control inputs of the system. Under this assumption, the motion of the two-wheeled mobile robot is determined by the following equation derived from (13) and (14):

$$\frac{\mathrm{d}z}{\mathrm{d}t} = Bu, \tag{18}$$

$$z = \begin{bmatrix} z_1 \\ z_2 \\ \theta \end{bmatrix}, \quad B = \begin{bmatrix} \cos\theta & 0 \\ \sin\theta & 0 \\ 0 & 1 \end{bmatrix}, \quad u = \begin{bmatrix} u_1 \\ u_2 \end{bmatrix},$$

where, as shown in Fig. 2, the state of the two-wheeled mobile robot is expressed in terms of the position of the mobile robot on the plane, z_1 and z_2, and the angle θ between the current direction of the mobile robot and the positive direction of the z_1 axis. The desired point is set to the origin. It is well known that this system is controllable at all points [11].

3.2. A controller based on Lyapunov control

We have proposed a method to design a controller for a three-dimensional two-input non-holonomic system without drift based on Lyapunov control [11, 12]. We introduce the following Lyapunov function:

$$V(z) = \frac{1}{2}\left(z_1^2 + z_2^2 + \theta^2\right). \tag{19}$$

The input vector is designed as follows:

$$u = \alpha(u_s + \beta u_a), \tag{20}$$

where α and β are positive constants:

$$u_s = -I_s B^T \nabla V, \tag{21}$$

$$u_a = -\frac{z_2}{g^2} I_a B^T \nabla V, \tag{22}$$

$$I_s = \begin{bmatrix} 1 & 0 \\ 0 & 1 \end{bmatrix}, \quad I_a = \begin{bmatrix} 0 & 1 \\ -1 & 0 \end{bmatrix},$$

$$g = |B^T \nabla V| = \sqrt{(z_1 \cos\theta + z_2 \sin\theta)^2 + \theta^2}, \tag{23}$$

$$\nabla = \left[\frac{\partial}{\partial z_1}, \frac{\partial}{\partial z_2}, \frac{\partial}{\partial \theta} \right]^T.$$

We define:

$$\frac{1}{g^2} B^T \nabla V = 0 \text{ at } B^T \nabla V = 0. \tag{24}$$

The term u_s in the input u, (21), moves the system so that the value of the Lyapunov function V decreases. Since the term u_s is zero on the line, $g = 0$, the system stops at a point on the line if the input u consists of only the term u_s. While, the term u_a in the input u, (22), moves the system so that the value of the Lyapunov function V is constant and keeps the system away from the line, $g = 0$.

Taking account of the characteristics of u_s and u_a, it is expected that the system with the input vector (20) moves away from the line, $g = 0$, reduces the value of the Lyapunov function $V(t)$ and converges to the origin as $V \to 0$. With the input vector (20), the derivative of the Lyapunov function is composed of a symmetric and an asymmetric bilinear form in the gradient vectors. We will call the control with this type of input an extended Lyapunov control. It is noteworthy that the coefficient of the asymmetric matrix is determined by Lie brackets which indicates the controllability of the system.

4. BEHAVIOR OF THE CONTROLLED SYSTEM

The basic equation (18) with the input (20) becomes

$$\frac{\mathrm{d}z}{\mathrm{d}t} = -\alpha B \left(I_s + \beta \frac{z_2}{g^2} I_a \right) B^T \nabla V. \tag{25}$$

Since the parameter α affects only the time scale, without loss of generality, the paremeter α can be set to 1.0. With (25), the derivative of $V(t)$ is computed as:

$$\begin{aligned} \dot{V} &= -\left(B^T \nabla V\right)^T \left(I_s + \beta \frac{z_2}{g^2} I_a \right) B^T \nabla V \\ &= -|B^T \nabla V|^2 \leqslant 0. \end{aligned} \tag{26}$$

The equilibrium points of the controlled system (25) are the points on the line, $g = 0$. From (23), the line, $g = 0$, coincides with the z_2 axis. Equation (26) shows

that the controlled system converges to the line. We will examine the stability of the points on the line. Since, on the line, the basic equation (25) is discontinuous, for the sake of analysis, we modify (25) as follows:

$$\dot{z} = -B\left(I_s + \beta \tanh\left(\frac{g^2}{\varepsilon}\right)\frac{z_2}{g^2} I_a\right) B^T \nabla V, \tag{27}$$

where ε is a small positive constant. Equation (27) becomes (25) as ε approaches zero. By linearizing (27) in the neighborhood of the equilibrium points, the stability of the system on the z_2 axis is revealed as follows:

$$\begin{cases} |z_2| < \sqrt{\dfrac{2\varepsilon}{\beta}} & \Longleftrightarrow \quad \text{stable focus} \\ \sqrt{\dfrac{2\varepsilon}{\beta}} < |z_2| < 2\sqrt{1+\dfrac{\varepsilon}{\beta}} & \Longleftrightarrow \quad \text{unstable focus} \\ |z_2| > 2\sqrt{1+\dfrac{\varepsilon}{\beta}} & \Longleftrightarrow \quad \text{unstable node.} \end{cases} \tag{28}$$

As the result, as ε approaches zero, the origin becomes the only stable equilibrium point of the system (27). Therefore, the origin becomes the only stable equilibrium point of the system (25).

The behavior of the system in the neighborhood of the origin is analyzed in detail [12]. First, in the region where $g^2 < O(\beta|z_2|)$, the following approximate solutions of the variables z and g are obtained:

$$\begin{aligned} z_1 &= g\cos(\omega_c t + \phi), \\ \theta &= g\sin(\omega_c t + \phi), \end{aligned} \tag{29}$$

$$z_2 = C_1 \mathrm{e}^{-\frac{\beta}{2}t}, \tag{30}$$

$$\begin{cases} \beta \neq 2: & g = \sqrt{C_2 \mathrm{e}^{-2t} + \frac{\beta}{2-\beta} C_1^2 \mathrm{e}^{-\beta t}} \\ \beta = 2: & g = \sqrt{(\beta C_1^2 t + C_2)\mathrm{e}^{-2t}} \end{cases}, \tag{31}$$

where C_1, C_2 and ϕ are constant, and $\omega_c = \beta z_2 / g^2$.

When $\beta < 4.0$, the system satisfies that $g^2 < O(\beta|z_2|)$ for all $t > 0$. As the time goes on, the amplitude of oscillation of the inputs u_1 and u_2 becomes a constant, $\sqrt{\beta(2-\beta)}$, if $\beta < 2.0$ and becomes 0 if $2.0 \leqslant \beta < 4.0$. The frequency of oscillation of the inputs, as the time goes on, becomes large exponentially. On the other hand, when $\beta > 4.0$, the system can not satisfy that $g^2 < O(\beta|z_2|)$ for all $t > 0$ and goes toward the region where $g^2 \geqslant O(\beta|z_2|)$.

Next, we consider the behavior of the system in the region where $g^2 \geqslant O(\beta|z_2|)$. In the region we obtain the equation for g as:

$$\dot{g} = -g. \tag{32}$$

From (32), we obtain:

$$g = C_3 e^{-t}, \tag{33}$$

where C_3 is constant. In this case, from (33), it follows that:

$$|z_2| \leqslant O(e^{-2t}). \tag{34}$$

When $\beta > 4.0$, the system converges to the origin and the magnitude of the inputs converges to 0. On the other hand, when $\beta < 4.0$, according to the initial value of the system, the system cannot satisfy that $g^2 \geqslant O(\beta|z_2|)$ for all $t > 0$ and may go toward the region where $g^2 < O(\beta|z_2|)$.

As a result of the analyses, the behavior of the controlled system is summarized as follows. The controlled system converges to the origin exponentially. The magnitude of the inputs u_1 and u_2 becomes 0 or a constant, as the time goes on. It should be noted that, if we set the parameter β such that $\beta > 4.0$, the system converges to the origin exponentially, the magnitude of the inputs converges to 0 and oscillation of the inputs with a high frequency can be avoided.

Based on the kinematic model, (18), numerical simulations were executed to check the analysis.

Case (a): The value of the parameter β is set to 1.0. The variables z_2 and g behave as the solutions, (30) and (31). Figure 3 shows the behavior of the system in the z_1z_2 plane. The amplitude of oscillation of the inputs, u_1 and u_2, converges to a constant, 1.0, as shown in Fig. 4.

Table 1.
Simulation cases (kinematic model)

	α	β	Initial value of z^T
Case (a)	—	1.0	(0.5, 1.0, 0.0)
Case (b)	—	5.0	(0.5, 1.0, 0.0)

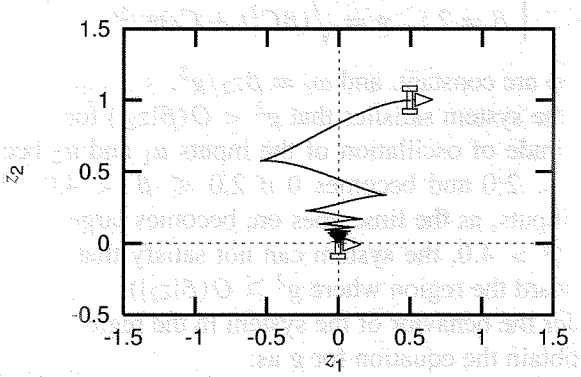

Figure 3. Motion of the system in the z_1z_2 plane [Case (a)].

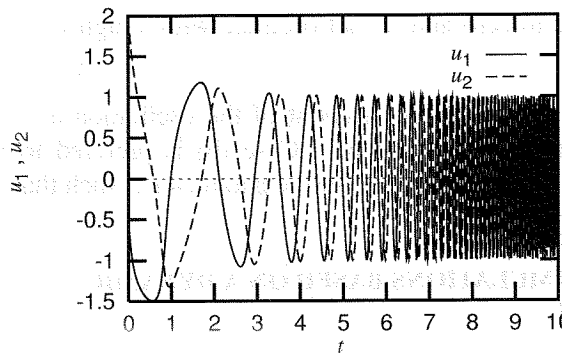

Figure 4. Time histories of u_1 and u_2 [Case (a)].

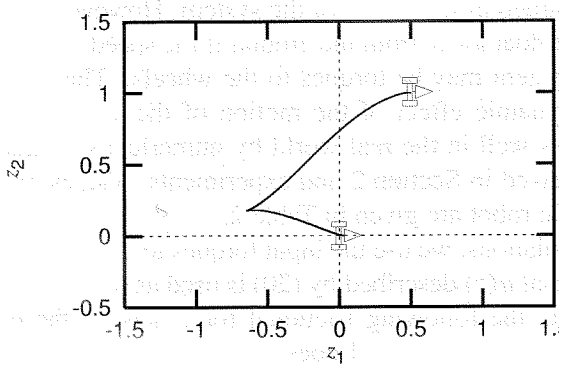

Figure 5. Motion of the system in the $z_1 z_2$ plane [Case (b)].

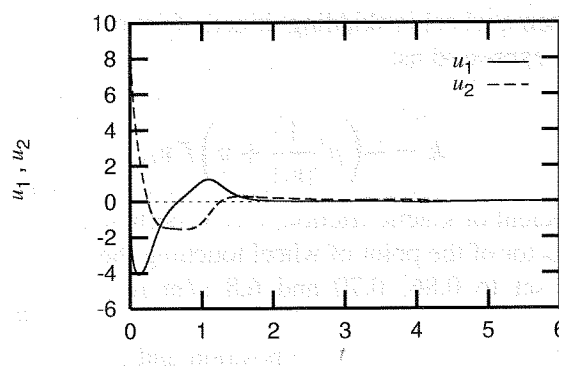

Figure 6. Time histories of u_1 and u_2 [Case (b)]

Case (b): The value of the parameter β is set to 5.0. Figure 5 shows the motion of the system in the $z_1 z_2$ plane. In this case, the system moves to the neighborhood of the desired point after two large switch-backs, and, in the neighborhood of the origin, converges to the origin exponentially without the oscillation of the variables z_1 and θ. The time history of variable g matches the solution, (33), very well. The inputs, u_1 and u_2,

converge to zero and do not oscillate with a high frequency as shown in Fig. 6.

From the above results, taking account of the oscillation and the magnitude of the inputs, the control performance in Case (b) is prefered to that of Case (a). Consequently, it is recommended to set the parameter β such that $\beta > 4.0$.

5. NUMERICAL SIMULATIONS BASED ON A DYNAMIC MODEL AND EXPERIMENTS

In Section 3 we designed a controller for a two-wheeled mobile robot under the condition that the wheels do not skid at all, and translational velocity u_1 and angular velocity u_2 are regarded as the inputs of the system. However, in the real world, the wheels may skid or float away from the ground if the speed of the motion is fast and the inputs of the system may be torques to the wheels. Therefore, in this section, we examine the dynamic effect of the motion of the system and check whether the controller works well in the real world by numerical simulations based on the dynamic model derived in Section 2 and experiments. Values of parameters of the two-wheeled mobile robot are given in Table 2.

In numerical simulations, we use the input torques to the wheels described by (17) where the input signal $u(z)$ described by (20) is used as referenced velocities $\hat{u}_1$ and $\hat{u}_2$. We assume that the following frictional force acts on the point of the wheel touching the ground. When a wheel does not skid, static friction acts on the point and the frictional force is up to the maximum static frictional force μF, where μ is a coefficient of static friction and F is the normal reaction force exerted on the point of wheel. When a wheel is skidding, kinetic friction acts on the point and the frictional force $\boldsymbol{k}$ is expressed as:

$$\boldsymbol{k} = -\left(\mu' \frac{1}{|\boldsymbol{v}_s|} + \nu\right) F \boldsymbol{v}_s, \tag{35}$$

where μ' is a coefficient of kinetic friction, ν is a coefficient of viscous friction and $\boldsymbol{v}_s$ is the velocity vector of the point of wheel touching the ground. The parameters, μ, μ' and ν, are set to 0.86, 0.70 and 6.8 s/m respectively, by preliminary measurements.

In experiments, as shown in Fig. 7, the position and attitude of the mobile robot on the ground are measured by a CCD camera, and the referenced velocities $\hat{u}_1$ and $\hat{u}_2$ are generated by personal computer. The vision system using the CCD camera provides position and attitude of the robot at a rate of 30 Hz. The range of view is about 2.2 m $\times$ 1.6 m and the measurement error in the position is less than about 2.0 cm. Each wheel is driven by a DC motor of which the rotational velocity is controlled by a PWM signal without using a feedback control. We adjust the parameters K_t in (17) and α in (20) so that the speed of the motion of the body in numerical simulations is consistent with the one in experiments.

Table 2.
Values of system parameters

Main body	length	25 (cm)
	width	15 (cm)
	height	6.5 (cm)
	mass	1.48 (kg)
Wheel	diameter	6.5 (cm)
	mass	0.081 (kg)

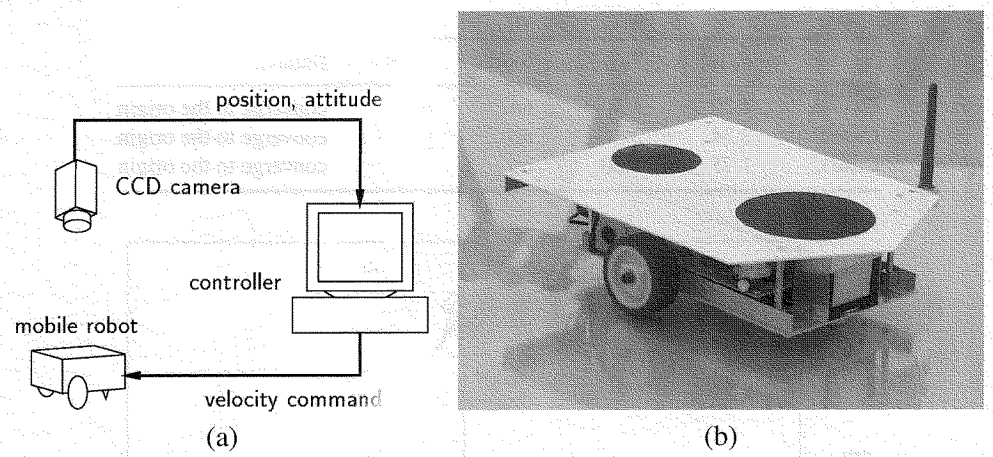

Figure 7. The architecture of the hardware equipment. (a) Total system. (b) Mobile robot.

We executed numerical simulations based on the dynamic model, (13) and (14), and experiments in three cases, Case A, B and C. Initial values of the state variable z and the parameters α and β in (20) are summarized as in Table 3. As the parameter α becomes large, the referenced velocities $\hat{u}_1$ and $\hat{u}_2$ are larger and the dynamic effect of the motion of the system becomes more crucial. The simulation results are shown in Figs 8–10 where the solid line shows the trajectory of the system in the z_1z_2 plane in a numerical simulation based on the dynamic model and the dashed line shows the trajectory in an experiment. The results are summarized in Table 4, where T_s is the time when the robot reached the first switch-back point from the initial point in numerical simulations and T_e is the time in experiments. These times imply the speeds of the motion of the body in numerical simulations and in experiments.

In Case A, since the motion of the system is slow, the wheels do not skid at all and the bar on the body or the wheels do not float away from the ground. In Fig. 8, the dash-dotted line shows the trajectory of the system in the z_1z_2 plane in the numerical simulation based on the kinematic model. The error in the trajectories of the two types of simulation arises from the force of inertia in the dynamic model and depends on the delay time in the loop, (17). The trajectory of the system in

Table 3.
Simulation cases (dynamic model)

	α	β	Initial value of z^T
Case A	0.175	5.0	(0.0, 1.0, −1.0)
Case B	0.3	5.0	(0.0, 1.0, −1.0)
Case C	0.42	5.0	(0.0, 1.0, −1.0)

Table 4.
Results of numerical simulations and experiments

	T_s [s]	T_e [s]	Skid	Float	Behavior
Case A	4.29	4.30	no	no	converge to the origin
Case B	2.34	2.36	no	yes	converge to the origin
Case C	1.78	1.80	no	yes	converge to the origin

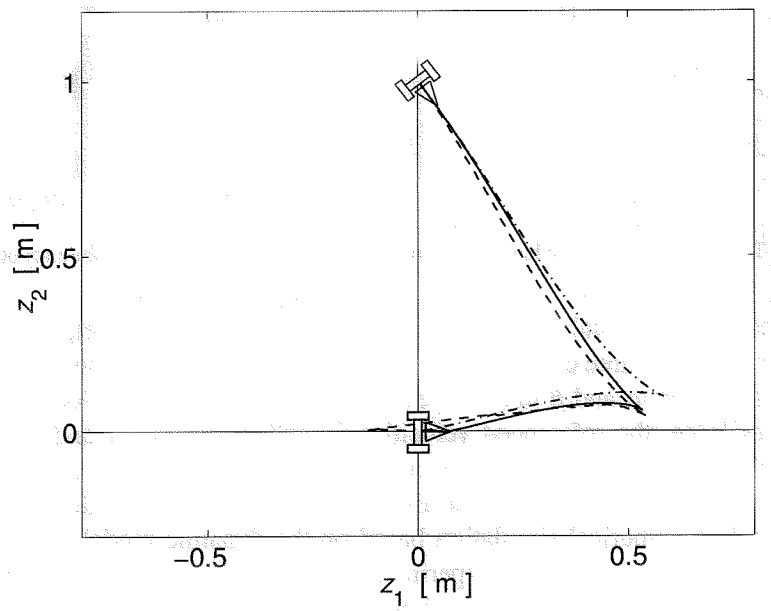

Figure 8. Motion of the system in the $z_1 z_2$ plane (Case A): kinematic model (dash-dotted), dynamic model (solid) and experiment (dashed).

the experiment shown by the dashed line agrees well with the one in the simulation based on the dynamic model.

In Case B, the motion of the system is faster than in Case A. As shown by the solid line in Fig. 9, when the system performs the first switch-back near $z_1 = 0.54$, it reaches further in the negative direction of the z_2 axis than in Case A. This is the effect of the force of inertia. The effect also appears in the experimental result

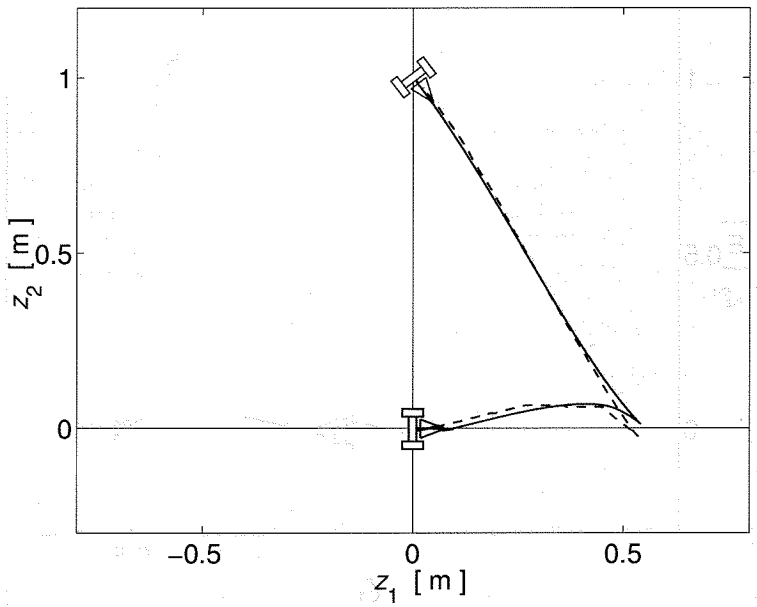

Figure 9. Motion of the system in the $z_1 z_2$ plane (Case B): dynamic model (solid) and experiment (dashed).

which is shown by the dashed line. Moreover, in both the numerical simulation based on the dynamic model and the experiment, the bar attached on the body floats away from the ground near the initial point. In the numerical simulation, the bar is floating while the system goes ahead about 0.3 cm in the forward direction from the initial point. In the experiment, the bar is floating while the system goes ahead about 6.0 cm. These results differ in degree, but both show that the dynamic effect, the float of the bar, happens as the motion of the system becomes faster.

In Case C, the motion of the system is faster than in Case B. In this case, the effect of the force of inertia is larger than in Case B. When the system performs the first switch-back near $z_1 = 0.55$, it reaches further in the negative direction of the z_2 axis than in Case B. Moreover, the bar attached on the body floats away from the ground near the initial point for a while. In both the numerical simulation based on the dynamic model and the experiment, the bar is floating while the system goes ahead about 40 cm in the forward direction from the initial point, which is shown by the dotted line in Fig. 10.

From the above results, if the value of the parameter α is small, it is proper to design the controller based on the kinematic model. However, as the value of the parameter α becomes larger, the difference between the real motion of the controlled system and the motion of the system in the kinematic model is more remarkable because of the effect of the force of inertia. Nevertheless, as shown by the above numerical simulations and experiments, the dynamic effect fades out as time advances and the system moves toward the desired state. The following two reasons why the designed controller (20) is robust against such dynamic effect may

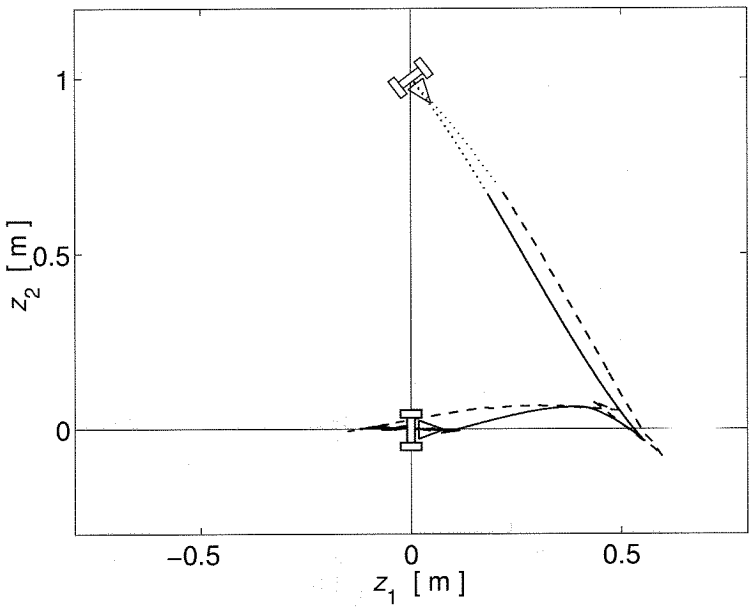

Figure 10. Motion of the system in the $z_1 z_2$ plane (Case C): dynamic model (solid) and experiment (dashed).

be considered. One is that the controller is designed based on Lyapunov control by using the Lyapunov function described by (19) and prevents the system from diverging further from the desired point. The other is that the controller is a state feedback one and makes the system go toward the desired point from any initial point. From a practical point of view, it is recommended to set the parameters of the controller (20), α and β, as follows. First, parameter β should be determined so that the controller generates an acceptable path of the robot in the $z_1 z_2$ plane based on the kinematic model. In order to avoid oscillation of the inputs and make the magnitude of the inputs converge to zero, parameter β must satisfy $\beta > 4.0$. Next, the parameter α should be determined so that the real motion of the system is not remarkably different from the motion of the system based on the kinematic model. The dynamic effect which causes the difference depends on coefficients of friction, and the parameters of the robot such as inertia and mass. Therefore, the parameter α should be determined according to the coefficients, the parameters and the initial values of the system.

6. CONCLUSIONS

In this paper, we designed a controller for a two-wheeled mobile robot and analyzed whether the designed controller works well in the real world by numerical simulations and experiments. In the real world, the wheels may skid on the ground or float away from the ground according to the rolling motion of the body. We

derived a dynamic model of a two-wheeled mobile robot and transformed it to a kinematic model under certain assumptions. Then, we designed a controller for the kinematic model by extending Lyapunov control and verified that the designed controller works well in the real world by numerical simulations based on the dynamic model and experiments.

REFERENCES

1. C. Samson, Control of chained systems application to path following and time-varying point-stabilization of mobile robots, *IEEE Trans. Automatic Control* **40** (1), 64–77 (1995).
2. O. J. Sørdalen and O. Egeland, Exponential stabilization of nonholonomic chained systems, *IEEE Trans. Automatic Control* **40** (1), 35–49 (1995).
3. R. T. M'Closkey and R. M. Murray, Exponential stabilization of driftless nonlinear control systems using homogeneous feedback, *IEEE Trans. Automatic Control* **42** (5), 614–628 (1997).
4. H. Khennouf and C. Canudas de Wit, Quasi-continuous exponential stabilizers for nonholonomic systems, in: *Proc. IFAC 13th World Congr.*, San Francisco, CA, pp. 2b–174 (1996).
5. A. Astolfi, Discontinuous control of nonholonomic systems, *Syst. Control Lett.* **27**, 37–45 (1996).
6. A. Astolfi, Exponential stabilization of a wheeled mobile robot via discontinuous control, *J. Dyn. Syst. Meas. Control* **121** (1), 121–125 (1999).
7. F. Bullo and R. M. Murray, Experimental comparison of trajectory trackers for a car with trailers, in: *Proc. IFAC 13th World Congr.*, San Francisco, CA, pp. 407–412 (1996).
8. S. Sekhavat, F. Lamiraux, J. P. Laumond, G. Bauzil and A. Ferrand, Motion planning and control for Hilare pulling a trailer: experimental issues, in: *Proc. IEEE Int. Conf. on Robotics and Automation*, Albuquerque, NM, pp. 3306–3311 (1997).
9. K. Ishikawa, K. Fujimoto and T. Sugie, Feedback control of two-wheeled vehicle based on generalized canonical transformation, in: *Proc. 43rd Ann. Conf. of ISCIE*, Osaka, Japan, pp. 629–630 (1999) (in Japanese).
10. R. T. M'Closkey and R. M. Murray, Experiments in exponential stabilization of a mobile robot towing a trailer, in: *Proc. Am. Control Conf.*, Baltimore, MD, pp. 988–993 (1994).
11. K. Tsuchiya, T. Urakubo and K. Tsujita, A motion control of a space manipulator by a generalized Lyapunov control, in: *Proc. ISAS 8th Workshop on Astrodynamics and Flight Mechanics*, Sagamihara, Japan, pp. 36–41 (1998).
12. K. Tsuchiya, T. Urakubo and K. Tsujita, Motion control of a non-holonomic system based on the Lyapunov control method, *J. Guidance Control Dyn.* (in press).

ABOUT THE AUTHORS

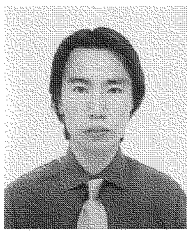

Takateru Urakubo received the BE and ME degrees in Aeronautics and Astronautics Engineering from Kyoto University in 1996 and 1998, respectively. He is a Doctoral candidate at the same university. His research interests are in non-linear control and autonomous robots. He is a member of the RSJ and SICE.

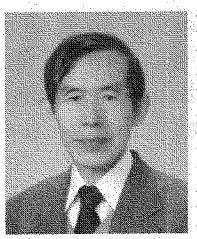

Kazuo Tsuchiya received the BE and ME degrees in Aeronautics and Astronautics Engineering from Kyoto University in 1966 and 1968, respectively, and the DE degree from the same university in 1974. From 1968 to 1990, he was a Senior Scientist at the Center Research Laboratory of Mitsubishi Electric Corporation. From 1990 to 1995, he was a Professor in the Department of Computer Controlled Machinery, Osaka University. Since 1995, he has been a Professor in the Department of Aeronautics and Astronautics, Kyoto University. His research interests are in space engineering and non-linear system theory. He is a member of the RSJ, SICE, AIAA, etc.

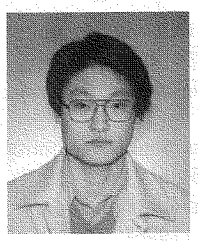

Katsuyoshi Tsujita received the BE and ME degrees in Engineering from Osaka University in 1991 and 1993, respectively. He served as a Research Associate of the Department of Computer Controlled Machinery, Osaka University from 1993 to 1995. He is now a Research Associate of the Department of Aeronautics and Astronautics, Kyoto University. His research interests are distributed autonomous robotic systems, locomotion robots, flexible mechanisms and control theory. He is a member of the RSJ and JSME.